

Supporting Information

Approaching 100% Selectivity at Low Potential on Ag for Electrochemical CO₂ Reduction to CO Using a Surface Additive

Aya K. Buckley,^{1,2,3,‡} Tao Cheng,^{4,5,‡} Myoung Hwan Oh,^{1,6} Gregory M. Su,^{7,8} Jennifer Garrison,^{1,2,3} Sean W. Utan,^{1,2,3} Chenhui Zhu,⁷ F. Dean Toste,^{1,2,3,} William A. Goddard III,^{5,*} Francesca M. Toma^{1,2,*}.*

¹Joint Center for Artificial Photosynthesis, Lawrence Berkeley National Laboratory, 1 Cyclotron Road, Berkeley, CA 94720, USA.

²Chemical Sciences Division, Lawrence Berkeley National Laboratory, 1 Cyclotron Road, Berkeley, CA 94720, USA.

³Department of Chemistry, University of California, Berkeley, CA 94720, USA

⁴Institute of Functional Nano & Soft Materials (FUNSOM), Jiangsu Key Laboratory for Carbon-Based Functional Materials & Devices, Joint International Research Laboratory of Carbon-Based Functional Materials and Devices, Soochow University, 199 Renai Road, Suzhou, 215123, Jiangsu, PR China

⁵Joint Center for Artificial Photosynthesis and Materials and Process Simulation Center; California Institute of Technology, Pasadena CA, 91125, USA

⁶Department of Energy Technology, Korea Institute of Energy Technology, Naju 58322, Republic of Korea

⁷Advanced Light Source, Lawrence Berkeley National Laboratory, 1 Cyclotron Road, Berkeley, CA 94720, USA

⁸Materials Sciences Division, Lawrence Berkeley National Laboratory, 1 Cyclotron Road, Berkeley, CA 94720, USA

[§]These two authors equally contributed to the manuscript

^{*}Corresponding authors: fdtoste@berkeley.edu, wag@caltech.edu, fmtoma@lbl.gov

Experimental and Theoretical Procedures

Materials

All chemicals were obtained from commercial suppliers and used without further purification, unless otherwise noted. Silver foil (1.0 mm thick, 99.9985%) was purchased from Alfa Aesar. Carbon dioxide (99.995%) was obtained from Praxair. Hexadecyltrimethylammonium bromide (**1-C16**, 98%) was obtained from Spectrum Chemical. Dihexadecyldimethylammonium bromide (**2-C16**, 97%), didecyldimethylammonium bromide (**2-C10**, 98%), and trimethyldecylammonium bromide (**1-C10**, 98%) were purchased from Sigma-Aldrich. Selemion AMV anion-exchange membrane was purchased from AGC Engineering Co., LTD.

Instrumentation

Gas chromatography (GC) data was collected on a multiple gas analyzer #5 from SRI Instruments. NMR spectra were recorded on a Bruker Avance III 500 MHz spectrometer. Electrochemical measurements were conducted using a BioLogic SP300 potentiostat.

Electrode preparation and electrochemical measurements

Ag foil was mechanically polished (1200G Wetordry sandpaper, 3M) and rinsed with water before use. To prepare modified Ag surfaces, 0.027 mmol of the organic species was dissolved in iPrOH (1 mL), and 100 μ L of this solution was drop cast onto the Ag foil, yielding to an estimated thickness of ~2-3 nm. Once dry, 100 μ L of Nafion solution (1 μ L of commercial Nafion solution per mg of organic species added to 1 mL iPrOH) dropped cast onto the Ag surface.

The prepared electrodes were placed in a two-compartment flow cell, fabricated from a reported design,¹ and electrochemical experiments were conducted as previously described.² Product distribution data was determined via chronoamperometry experiments conducted for 35 minutes, and the average of data from three independently prepared electrodes are reported.

Computational Details

All the ReaxFF MD simulations were carried out using LAMMPS Molecular Dynamics Simulator. The simulation models consist of 1440 Ag atoms [4 \times 18 \times 20 Cu(111) surface], 2000 water molecules, 26 polymers, and 26 Br anions making the system neutral. The total number of atoms per periodic cell is 9519, 10026, 9675, and 10011.

The dimension of the periodic box for the simulations is 4.60 nm \times 4.42 nm \times 5.00 nm.

Energy minimization was carried out first to relax the interface structure with a force convergence criteria of 10⁻⁶ kcal/mol \cdot \AA .

Constant temperature, constant volume (NVT) simulations were carried out at room temperature (298K) with a Nose-Hoover thermostat for 5 ns with a time step of 0.25 fs. The surface tensions of the solid/liquid interface (γ_{SL}) were calculated from molecular dynamics simulations.

GIWAXS Experiments

Grazing incidence X-ray scattering (GWAXS) experiments were performed at bending magnet beamline 7.3.3 at the Advanced Light Source (ALS).³ The X-ray energy was 10 keV. A 0.14° incidence angle was used, and exposure times were between 0.2-1.0 s. The sample-to-detector distance was 28 cm, and a silver behenate calibrant was used to determine beam center and sample-to-detector distance. A Pilatus 2M area detector was used for 2D diffraction pattern collection. Samples were enclosed in a helium filled chamber to minimize air scattering. Data reduction was processed using the Nika software within Igor Pro.⁴

^1H NMR Analysis of Structural Stability of Cationic Modifiers during Electrochemical Measurements.

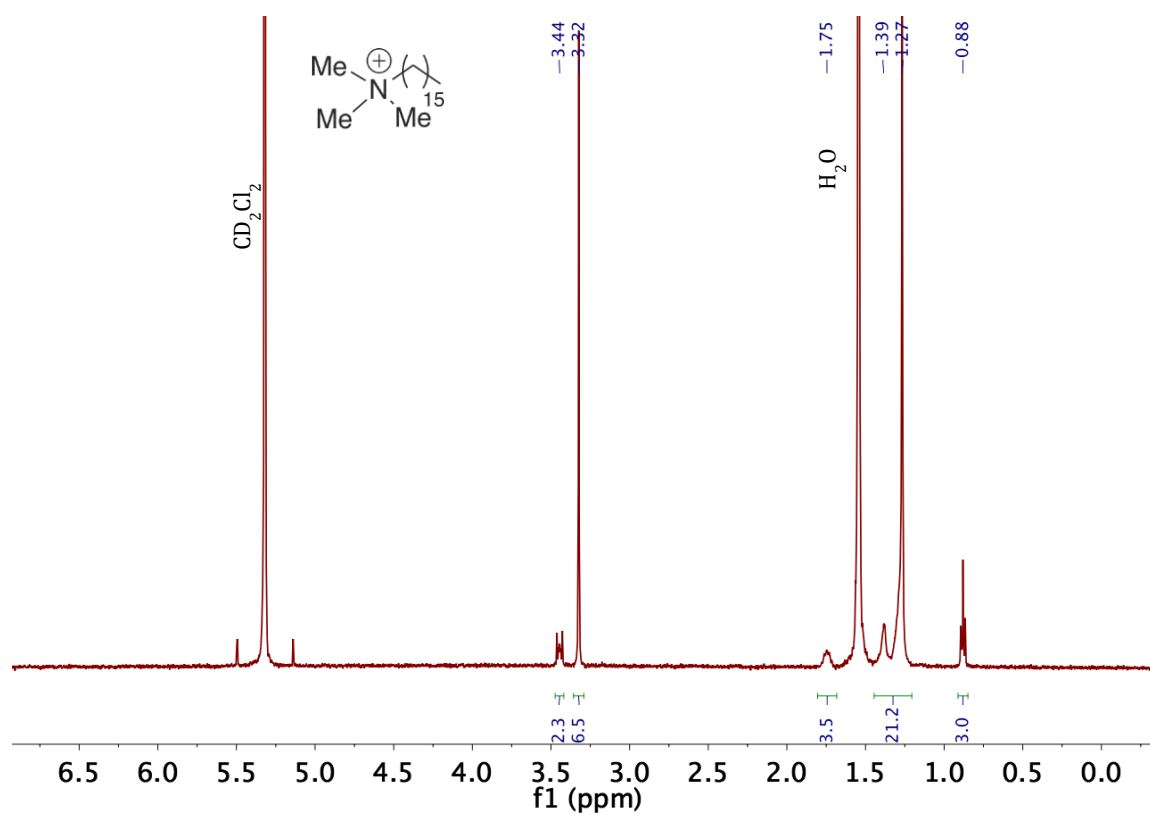


Figure S1. ^1H NMR of cetyltrimethylammonium bromide (**1**), rinsed from electrode after 35 minutes of chronoamperometry.

^1H NMR (500 MHz, CD_2Cl_2 , ppm): δ 3.44 (m, 2H), 3.32 (s, 9H), 1.75 (m, 2H), 1.39-1.27 (m, 26H), 0.88 (m, 3H).

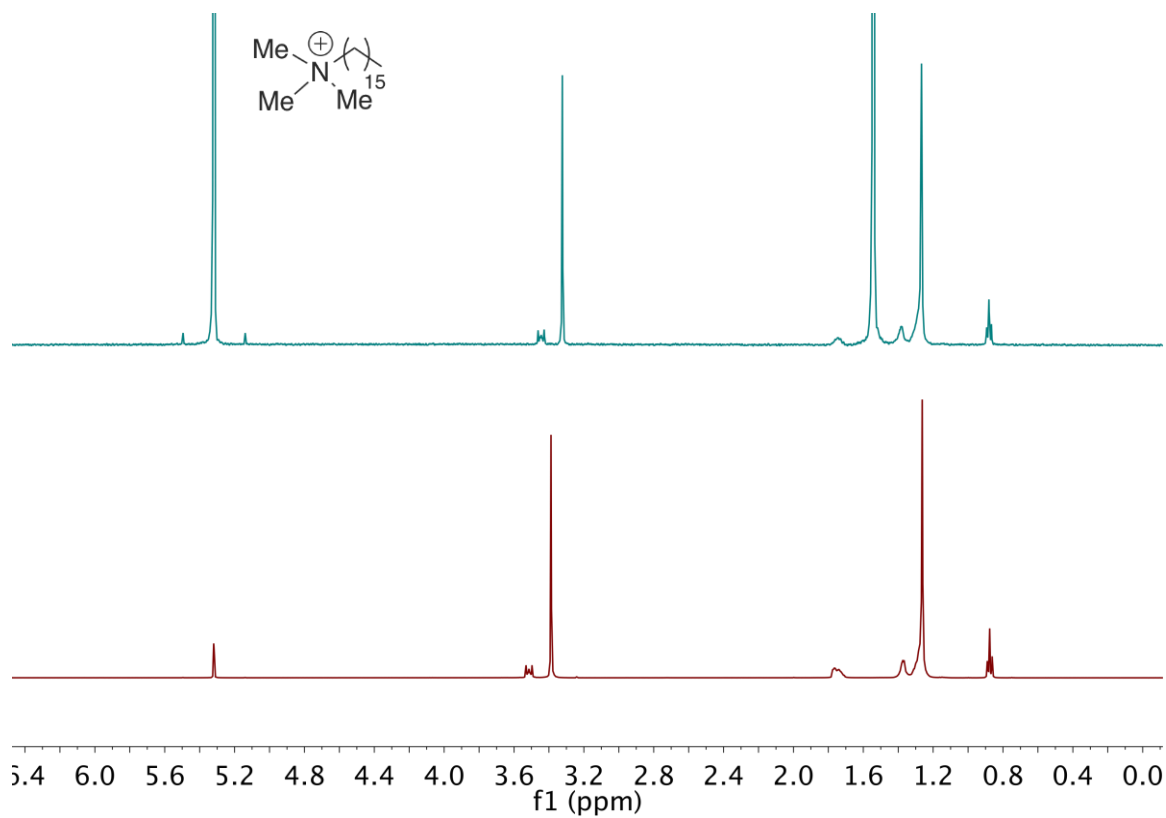


Figure S2. ^1H NMR of commercial cetyltrimethylammonium bromide (**1**) in CD_2Cl_2 (bottom), compared with a rinse of the electrode after 35 minutes of chronoamperometry, also in CD_2Cl_2 (top).

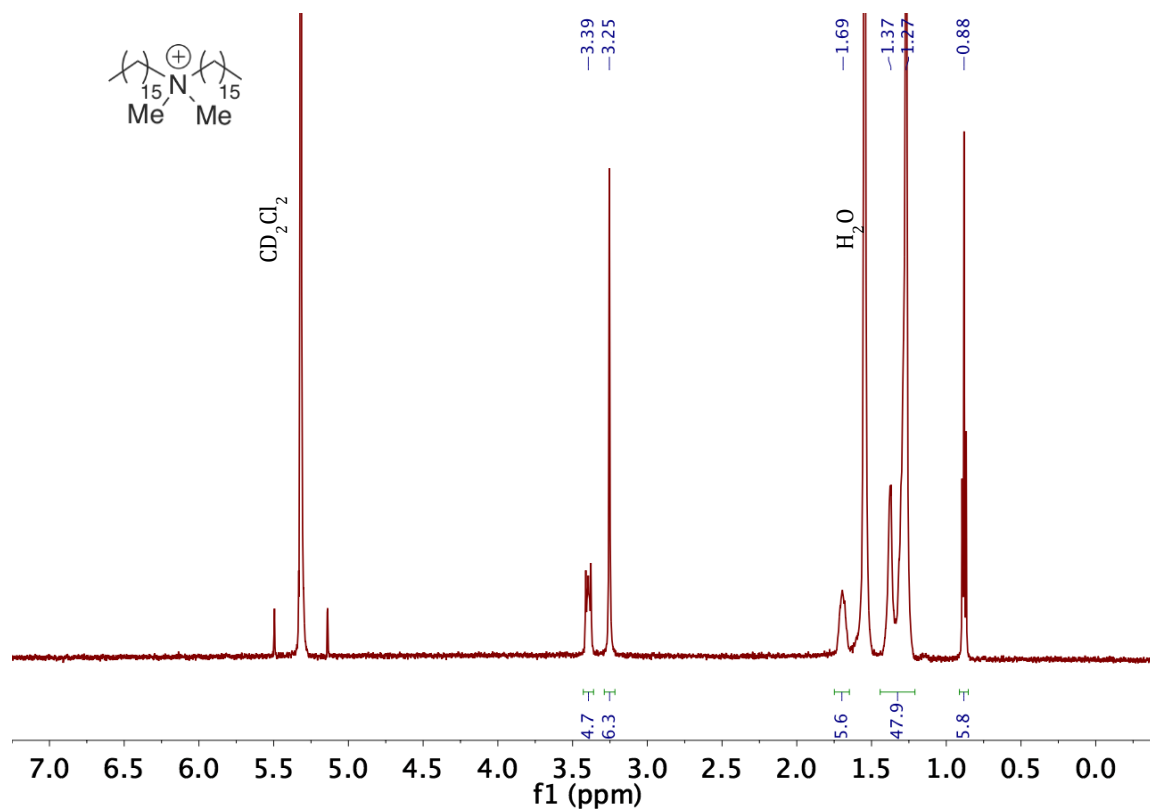


Figure S3. ¹H NMR of dihexacyldimethylammonium bromide (**2**), rinsed from electrode after 35 minutes of chronoamperometry.

¹H NMR (500 MHz, CD₂Cl₂, ppm): δ 3.39 (m, 4H), 3.25 (s, 6H), 1.69 (m, 4H), 1.37-1.27 (m, 52H), 0.88 (m, 6H).

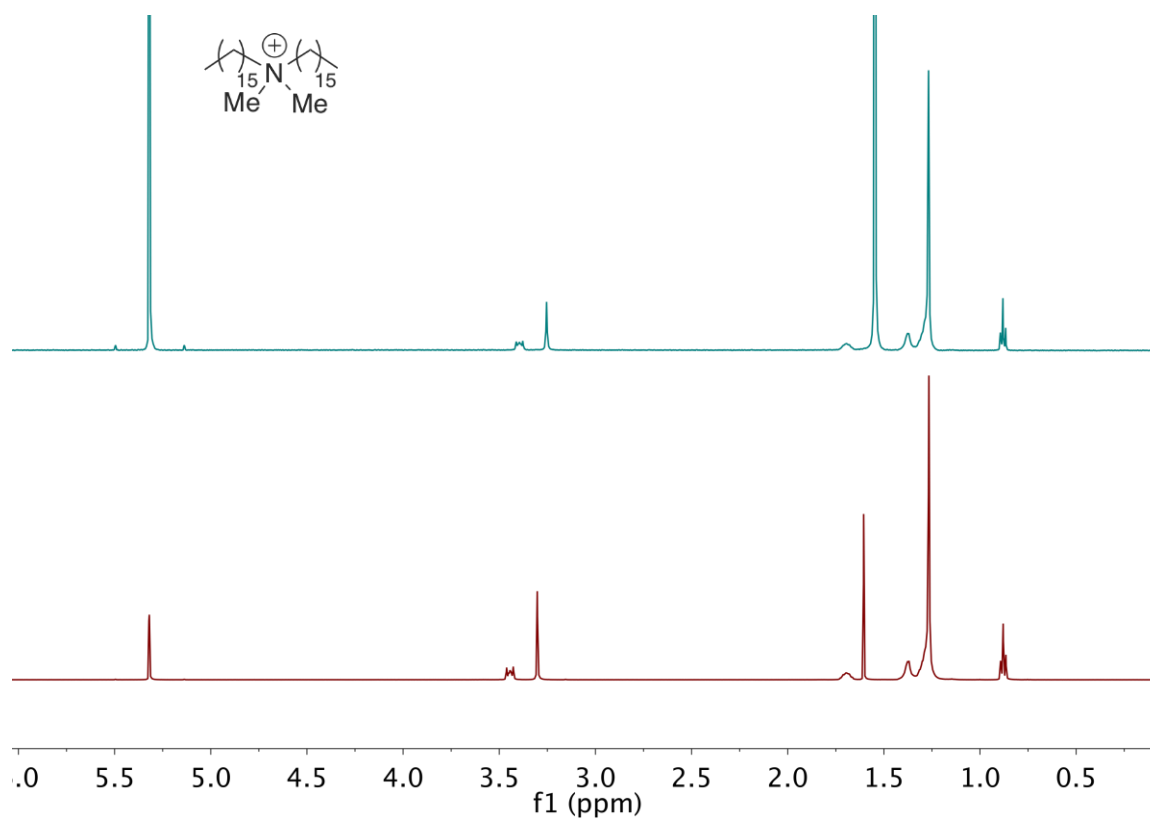


Figure S4. ^1H NMR of commercial dihexadecyldimethylammonium bromide (**2**) in CD_2Cl_2 (bottom), compared with a rinse of the electrode after 35 minutes of chronoamperometry, also in CD_2Cl_2 (top).

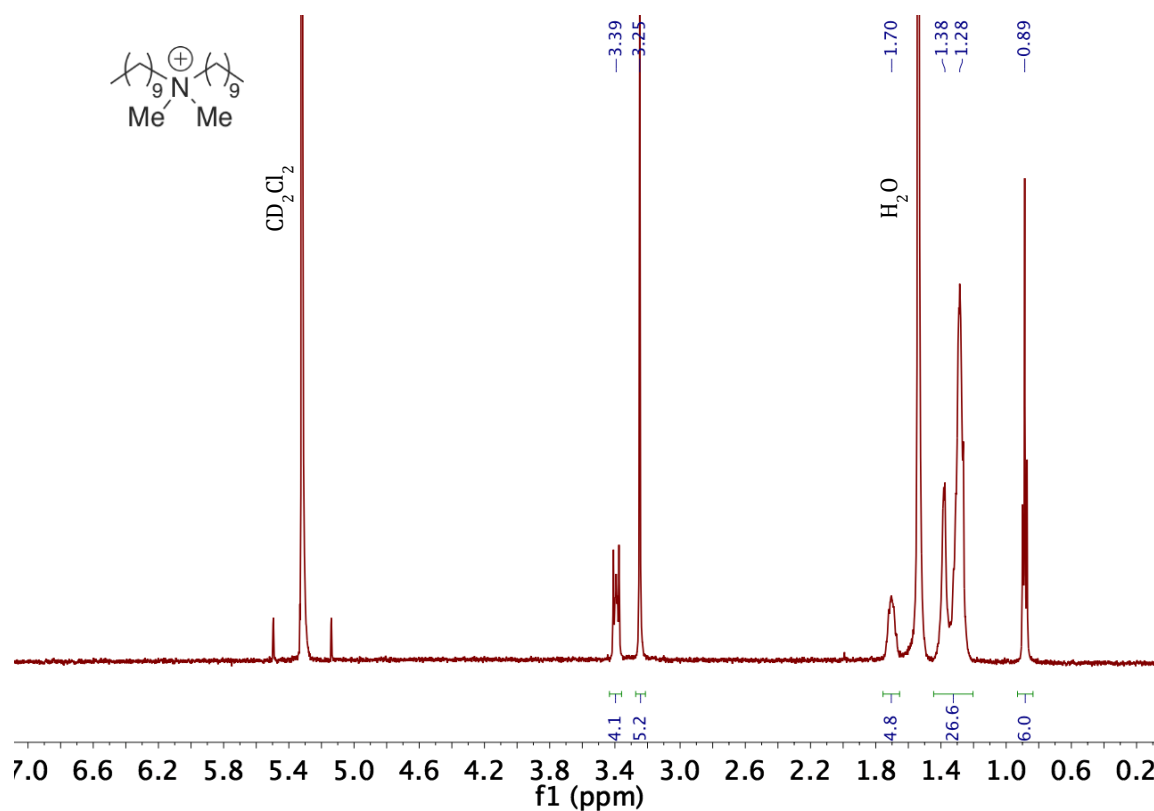


Figure S5. ^1H NMR of didecyldimethylammonium bromide (**3**), rinsed from electrode after 35 minutes of chronoamperometry.

^1H NMR (500 MHz, CD_2Cl_2 , ppm): δ 3.39 (m, 4H), 3.25 (s, 6H), 1.70 (m, 4H), 1.38-1.28 (m, 28H), 0.89 (m, 6H).

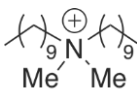


Figure S6. ^1H NMR of commercial didecyldimethylammonium bromide (**3**) in CD_2Cl_2 (bottom), compared with a rinse of the electrode after 35 minutes of chronoamperometry, also in CD_2Cl_2 (top).

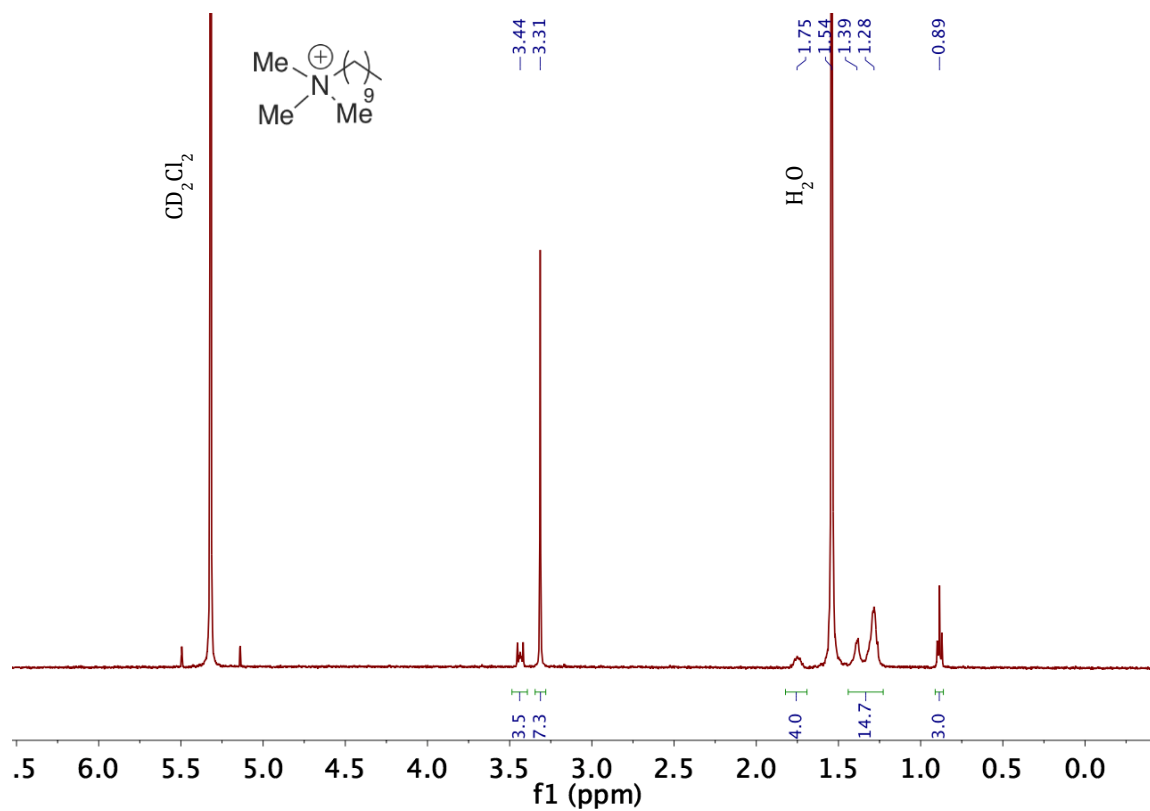


Figure S7. ^1H NMR of decyltrimethylammonium bromide (**4**), rinsed from electrode after 35 minutes of chronoamperometry.

^1H NMR (500 MHz, CD_2Cl_2 , ppm): δ 3.44 (m, 2H), 3.31 (s, 9H), 1.75 (m, 2H), 1.39-1.28 (m, 14H), 0.89 (m, 3H).

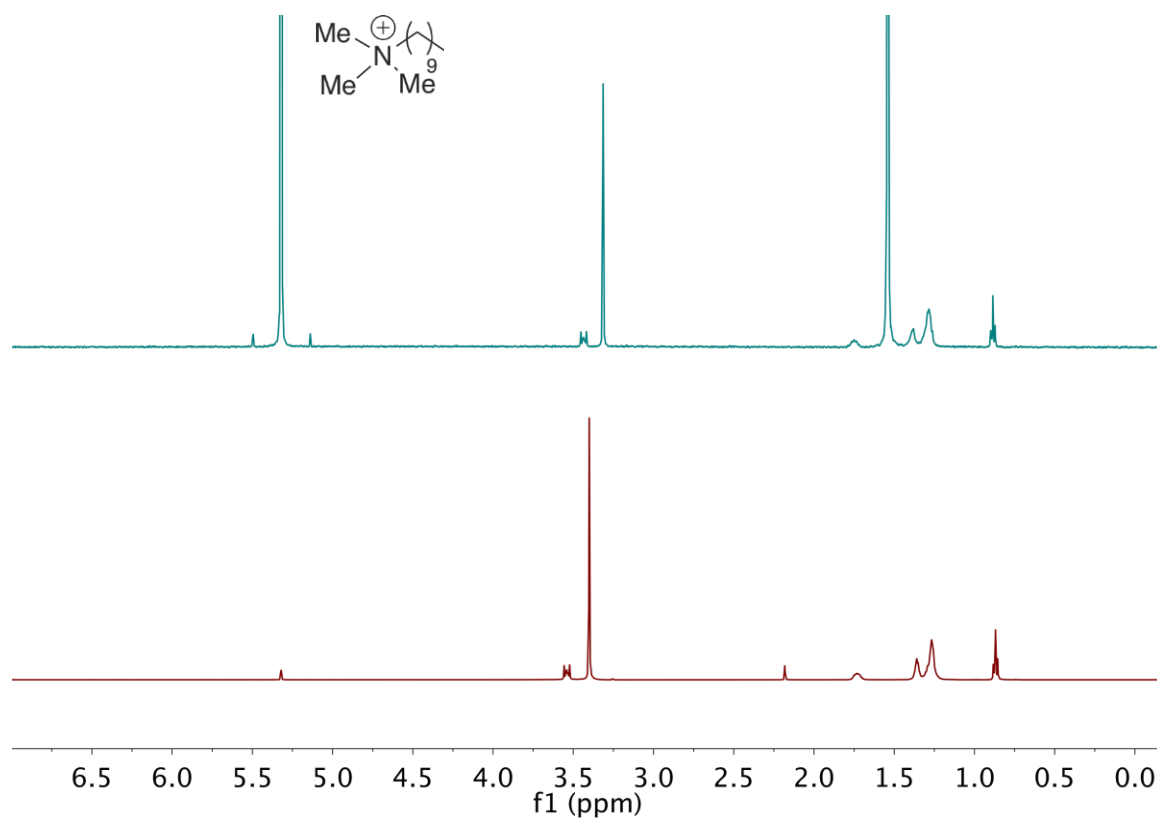


Figure S8. ^1H NMR of commercial decyltrimethylammonium bromide (**4**) in CD_2Cl_2 (bottom), compared with a rinse of the electrode after 35 minutes of chronoamperometry, also in CD_2Cl_2 (top).

ReaxFF MD Simulations of Functionalized Ag Surfaces

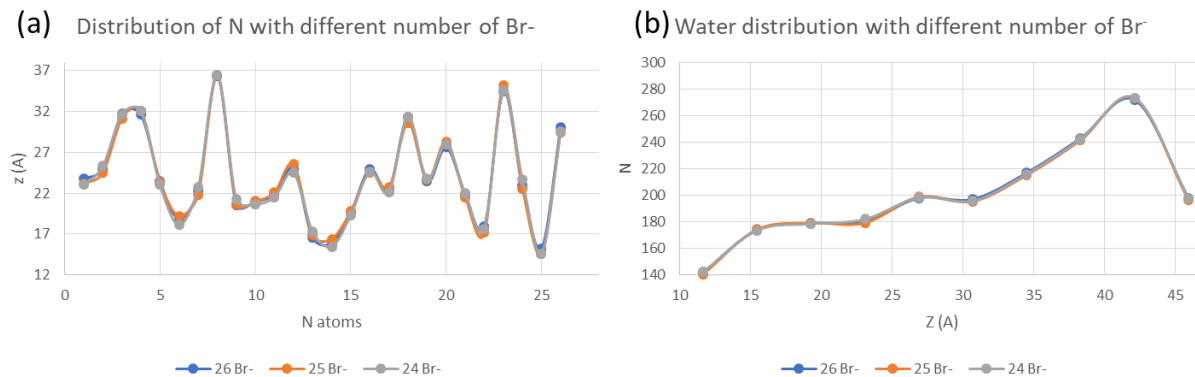


Figure S9. Distribution of N (a) and water (b) with 26 (blue), 25 (orange), and 24 (grey) Br⁻ of 2-C16.

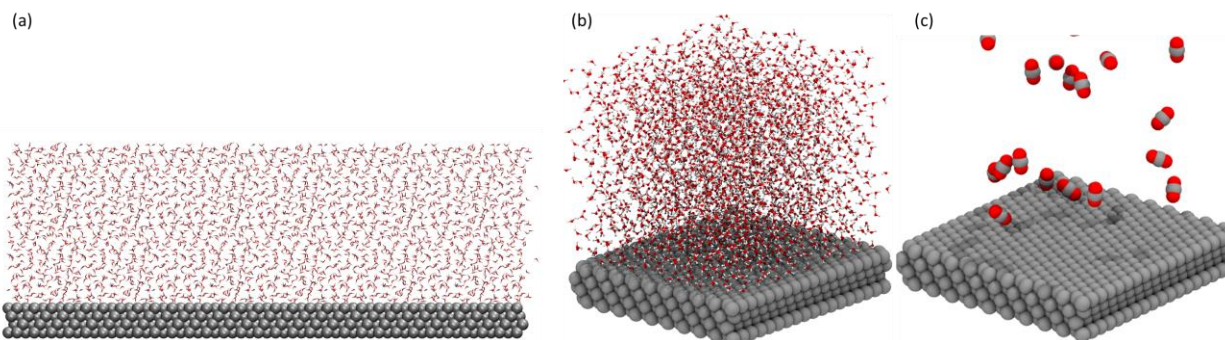


Figure S10. Snapshot of the interface between the bare Ag surface and (a) water, and CO₂, (b) water, (c) CO₂.

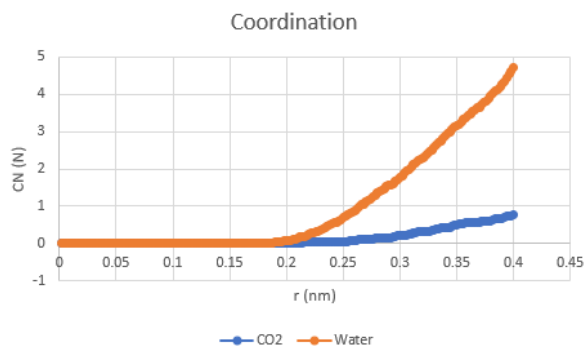


Figure S11. Coordination number (CN) of CO₂ itself and CO₂ with water. At a cutoff of 0.4 nm, the CN of CO₂ to CO₂ is 0.785, and the CN of CO₂ to water is 4.727.

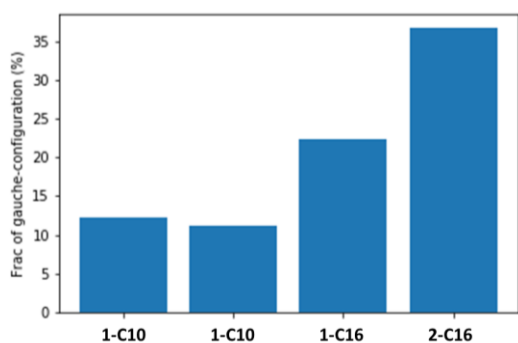


Figure S12. The fraction of trans-gauche conformations in the organic modifiers.

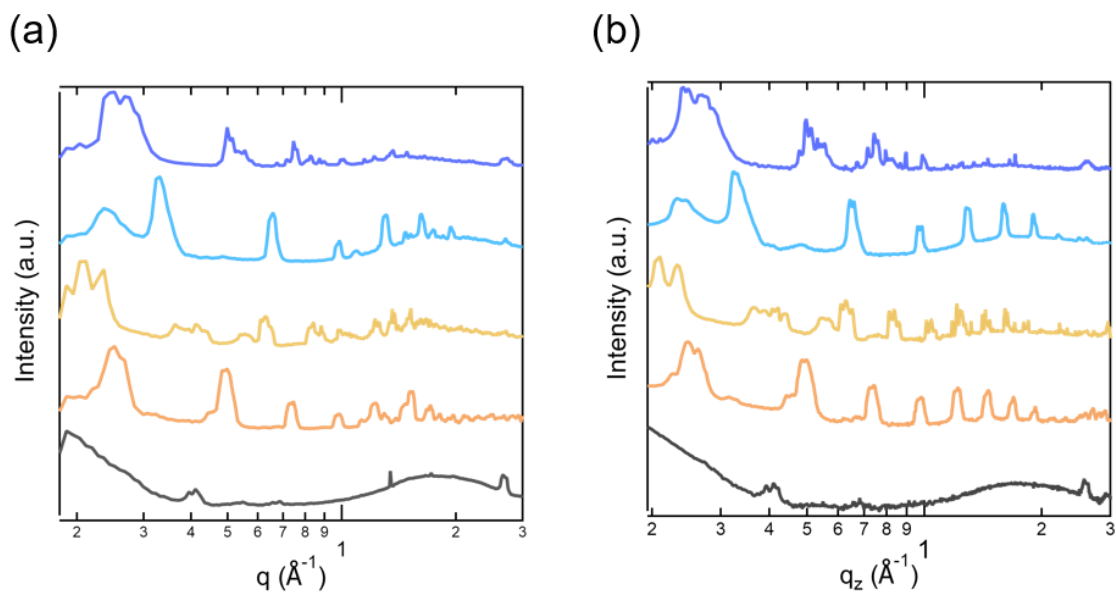
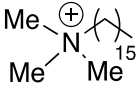
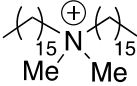
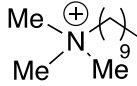
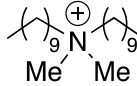


Figure S13. Reduced data is shown for (a) radially averaged intensity vs. q data and (b) nearly out-of-plane scattering data taken from vertical line cuts of the two-dimensional images reported in the main text at $q_{xy} = 0$. Scattering from the Ag-coated glass substrate is shown as the bottom black trace in (a) and (b).

The Contact Angle of Functionalized Ag Surfaces

Table S1: Ag surfaces in order of increasing hydrophobicity, compared to the selectivity of these surfaces for CO. Modified Ag surfaces were prepared by drop-casting at the same loading as for the chronoamperometry measurements. Contact angle measurements were obtained with 1 μ L droplets of water, and the average of at least four measurements is reported.

We find that surfaces with 1 and 2 have similar CO selectivities but very different hydrophilicities, suggesting that the interaction of the modifiers with the surrounding water is not the selectivity-determining factor.

Surface:	 1-C16	 2-C10	 1-C10	 2-C16	Ag foil
Contact angle:	4° \pm 1	54° \pm 3	15° \pm 2	11° \pm 1	69° \pm 1
CO selectivity:	90%	97%	48%	45%	25%
γ_{SL} (mN/m)	104.21	113.81	104.86	100.48	

Raw Data Used in the Figures

Table S2: Data plotted in Figure 1a. Error is reported as the standard error of the mean. Values and error bars are calculated from at least three trials.

Surface	H ₂ (%)	CO (%)
Ag	81.30 ±0.05	25.39 ±0.03
1-C16	6.59 ±0.05	89.81 ±0.02
2-C16	0.15 ±0.001	96.62 ±0.01
2-C10	53.87 ±0.04	44.71 ±0.04
1-C10	54.16 ±0.05	47.62 ±0.03

Table S3: Data plotted in Figure 1b. Error is reported as the standard error of the mean. Values and error bars are calculated from at least three trials.

Surface	H ₂ (mA/cm ²)	CO (mA/cm ²)
Ag	0.44 ±0.02	0.14 ±0.03
1-C16	0.04 ±0.03	0.71 ±0.14
2-C16	0.001 ±0.001	1.21 ±0.27
2-C10	0.05 ±0.002	0.04 ±0.01
1-C10	0.21 ±0.02	0.19 ±0.02

Table S4: Data plotted in Figure 3a (1-C16).

Z (nm)	Number of H ₂ O molecules
1.1307	134
1.5061	148
1.8815	184
2.2569	223
2.6323	256
3.0077	263
3.3831	267
3.7585	260
4.1339	224
4.5093	41

Table S5: Data plotted in Figure 3b (2-C16).

Z (nm)	Number of H ₂ O molecules
1.168	71
1.548	127
1.928	162
2.308	203
2.688	245
3.068	224
3.448	218
3.828	229
4.208	248
4.588	273

Table S6: Data plotted in Figure 3c (2-C10).

Z (nm)	Number of H₂O molecules
1.1635	142
1.5445	174
1.9255	179
2.3065	180
2.6875	198
3.0685	197
3.4495	217
3.8305	243
4.2115	272
4.5925	198

Table S7: Data plotted in Figure 3d (1-C10).

Z (nm)	Number of H₂O molecules
1.1182	87
1.4486	170
1.779	191
2.1094	225
2.4398	240
2.7702	249
3.1006	238
3.431	241
3.7614	241
4.0918	118

Table S8: Data plotted in Figure 4a (1-C16).

Z (nm)	Number of CO₂ molecules
1.01865	27
1.33515	6
1.65165	6
1.96815	9
2.28465	5
2.60115	6
2.91765	4
3.23415	5
3.55065	5
3.86715	8

Table S9: Data plotted in Figure 4b (2-C16).

Z (nm)	Number of CO₂ molecules
1.03564	45
1.38991	13
1.74417	11

2.09845	6
2.45271	5
2.80699	8
3.16125	4
3.51552	6
3.8698	6
4.22407	7

Table S10: Data plotted in Figure 4c (**2-C10**).

Z (nm)	Number of CO₂ molecules
1.01908	18
1.34444	4
1.6698	0
1.99516	0
2.32052	0
2.64588	0
2.97124	2
3.2966	2
3.62196	1
3.94732	3

Table S11: Data plotted in Figure 4d (**1-C10**).

Z (nm)	Number of CO₂ molecules
1.01559	14
1.30757	4
1.59955	1
1.89153	1
2.18351	3
2.47549	2
2.76747	4
3.05945	1
3.35143	1
3.64341	2

References for Supporting Information

1. Lobaccaro, P.; Singh, M. R.; Clark, E. L.; Kwon, Y.; Bell, A. T.; Ager, J. W. Effects of Temperature and Gas-Liquid Mass Transfer on the Operation of Small Electrochemical Cells for the Quantitative Evaluation of CO₂ Reduction Electrocatalysts. *Phys. Chem. Chem. Phys.* **2016**, *18*, 26777-26785.
2. Buckley, A. K.; Lee, M.; Cheng, T.; Kazantsev, R. V.; Larson, D. M.; Goddard III, W. A.; Toste, F. D.; Toma, F. M. Electrocatalysis at Organic-Metal Interfaces: Identification of Structure-Reactivity Relationships for CO₂ Reduction at Modified Cu Surfaces. *J. Am. Chem. Soc.* **2019**, *141*, 7355-7364.
3. Hexemer, A.; Bras, W.; Glossinger, J.; Schaible, E.; Gann, E.; Kirian, R.; MacDowell, A.; Church, M.; Rude, B.; Padmore, H. A SAXS/WAXS/GISAXS Beamline with Multilayer Monochromator *J. Phys. Conf. Ser.* **2010**, *247*, 012007
4. Ilavsky, J. Nika: software for two-dimensional data reduction. *J. Appl. Cryst.* **2012**, *45*, 324-328.